



**HAL**  
open science

# Multiple Crossed Isopolymorphism: Two-Component Systems $\text{CCl}_4 + \text{CBr}_2\text{Cl}_2$ and $\text{CBrCl}_3 + \text{CBr}_2\text{Cl}_2$ ; Inference of a Metastable Rhombohedral Phase of $\text{CBr}_2\text{Cl}_2$

María Barrio, Philippe Négrier, Josep Ll. Tamarit, Luis C. Pardo, Denise Mondieig

## ► To cite this version:

María Barrio, Philippe Négrier, Josep Ll. Tamarit, Luis C. Pardo, Denise Mondieig. Multiple Crossed Isopolymorphism: Two-Component Systems  $\text{CCl}_4 + \text{CBr}_2\text{Cl}_2$  and  $\text{CBrCl}_3 + \text{CBr}_2\text{Cl}_2$ ; Inference of a Metastable Rhombohedral Phase of  $\text{CBr}_2\text{Cl}_2$ . *Journal of Physical Chemistry B*, 2007, 111 (30), pp.8899-8909. 10.1021/jp071886x . hal-01553042

**HAL Id: hal-01553042**

**<https://hal.science/hal-01553042>**

Submitted on 24 Jul 2017

**HAL** is a multi-disciplinary open access archive for the deposit and dissemination of scientific research documents, whether they are published or not. The documents may come from teaching and research institutions in France or abroad, or from public or private research centers.

L'archive ouverte pluridisciplinaire **HAL**, est destinée au dépôt et à la diffusion de documents scientifiques de niveau recherche, publiés ou non, émanant des établissements d'enseignement et de recherche français ou étrangers, des laboratoires publics ou privés.



Distributed under a Creative Commons Attribution - NonCommercial - ShareAlike 4.0 International License

# Multiple Crossed Isopolymorphism: Two-Component Systems $\text{CCl}_4 + \text{CBr}_2\text{Cl}_2$ and $\text{CBrCl}_3 + \text{CBr}_2\text{Cl}_2$ ; Inference of a Metastable Rhombohedral Phase of $\text{CBr}_2\text{Cl}_2$

María Barrio,<sup>†</sup> Philippe Negrier,<sup>‡</sup> Josep Ll. Tamarit,<sup>\*,†</sup> Luis C. Pardo,<sup>§</sup> and Denise Mondieig<sup>§</sup>

*Departament de Física i Enginyeria Nuclear, E.T.S.E.I.B., Universitat Politècnica de Catalunya, Diagonal, 647, 08028 Barcelona, Catalonia, Spain, Centre de Physique Moléculaire, Optique et Hertzienne, UMR 5798 au CNRS-Université Bordeaux I, 351, cours de la Libération, 33405 Talence Cedex, France, and Experimental Physics V, Center for Electronic Correlations and Magnetism, University of Augsburg, 86135 Augsburg, Germany*

The phases diagrams of the two-component systems  $\text{CCl}_4 + \text{CBr}_2\text{Cl}_2$  and  $\text{CBrCl}_3 + \text{CBr}_2\text{Cl}_2$  have been determined by means of X-ray powder diffraction and thermal analysis techniques from the low-temperature ordered phase to the liquid state. The isomorphism relationship between the stable orientationally disordered (OD) face-centered cubic (FCC) phases of  $\text{CBrCl}_3$  and  $\text{CBr}_2\text{Cl}_2$  and the metastable OD FCC phase (monotropic behavior with respect to the OD rhombohedral stable phase) of  $\text{CCl}_4$  has been put into evidence throughout the continuous evolution of the lattice parameters and the existence of the two-phase equilibrium [FCC + L] for the whole range of composition in both two-component systems. This equilibrium interferes, for the  $\text{CCl}_4 + \text{CBr}_2\text{Cl}_2$  system, with a rhombohedral (R) plus liquid ([R + L]) equilibrium giving rise to a peritectic invariant. In addition, whatever the system, [R + FCC] equilibrium also interferes with the low-temperature equilibria between the low-temperature monoclinic (C2/c) phase and the OD R and FCC phases. In regards to the low-temperature monoclinic phases, isomorphism is evidenced, and by means of Rietveld profile refinement, any ordering of the molecules by varying the fractional occupancy of the halogen sites has been detected. The thermodynamic assessment, conducted by means of the concept of crossed isopolymorphism, coherently reproduces all the involved equilibria and provides a coherent set of data for the thermodynamic properties of nonexperimentally available phase transitions of pure compound  $\text{CBr}_2\text{Cl}_2$  which enables us to obtain the topological properties of its pressure–temperature phase diagram and to infer the existence of a high-pressure R phase for such a compound.

## 1. Introduction

Orientationally disordered (hereafter abbreviated by OD) crystalline phases show three-dimensional long-range order in respect to the molecular positions and extreme disorder in the orientational degrees of freedom of molecules at each lattice point. Such OD phases are typically found in “globular” compounds.<sup>1,2</sup> The halogenomethane compounds,  $\text{CX}_n\text{Y}_m$ , ( $n, m = 0, \dots, 4; n + m = 4; X, Y = \text{F}, \text{Cl}, \text{Br}, \text{I}$ ) are compounds formed by molecules of more or less globular shape, providing little steric hindrance for reorientational processes and, thus, giving rise to the existence of OD phases as introduced by Timmermans.<sup>1</sup>

The phase relations as a function of temperature at normal pressure for the compounds of the aforementioned family seem, however, quite different on account of the difference in size of the chlorine and bromine atoms.<sup>3–9</sup> Another family, closely related to the halogenomethane compound is that of methylchloromethane compounds,  $(\text{CH}_3)_{4-n}\text{CCl}_n$ ,  $n = 1, \dots, 4$ . The phase behavior of this family has been extensively studied.<sup>11–31</sup> As for the OD state, they exhibit a polymorphic nature such that at least two OD forms are involved, the symmetry of which

are rhombohedral (R) or cubic (FCC or SC). Upon cooling, compounds corresponding to  $n = 2, 3$ , and 4 solidify into a cubic phase [FCC for  $n = 3$  and 4, and simple cubic for  $n = 2$ ], and then transform to an OD R structure with further cooling. When heated, phase R melts without passing back through the cubic phase. When cooling is limited so that the cubic phase is formed, the cubic phase melts. Then, the cubic phase is metastable with respect to the former R phase and behaves monotonically at ordinary pressure. The melting pressure–temperature curve of these compounds ( $n = 2, 3$ , and 4) is rather convex, indicating that there should be no triple point involving liquid and R and cubic OD solid phases (at positive pressure), an evidence that we are dealing with a cubic metastable state at any pressure.<sup>7,11,23–25,32</sup> This case, which is known as overall monotropic behavior, is schematized in the pressure–temperature (p–T) diagram of Figure 1a. For such a case, R–FCC–L triple point is invariably located in the negative pressure domain.

As for the remaining compound,  $n = 1$ , only one face-centered cubic (FCC) OD phase is observed at normal pressure. Nevertheless, when polymorphism analysis is extended to the high-pressure domain, a new OD phase, which has been demonstrated to be of rhombohedral symmetry, appears in the positive pressure domain.<sup>33,34</sup> It means then that intermolecular interactions combined with steric conditions reach the necessary requirements to stabilize the R phase at high pressures. It should be noticed that the R–FCC–L triple point can make then a

\* Corresponding author phone: +34 934016564; fax: +34 93401 18 39; e-mail: jose.luis.tamarit@upc.edu.

<sup>†</sup> Universitat Politècnica de Catalunya.

<sup>‡</sup> CNRS-Université Bordeaux I.

<sup>§</sup> University of Augsburg.

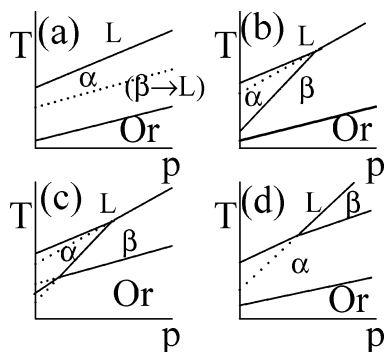


**Figure 1.** Temperature–pressure diagrams involving stable (continuous lines) and metastable (dashed lines) two-phase equilibria involving liquid (L), OD  $\alpha$  and  $\beta$ , and ordered (Or) phases.

physical appearance in the positive pressure domain, as displayed in Figure 1c, or in the negative domain, as for  $n = 1$ .<sup>34</sup>

As for the halogenomethane  $\text{CBrCl}_3$  compound, the enantiotropic behavior between a cubic (FCC) and R phases has been recently stated at ordinary pressure<sup>3–5</sup> and extension at high-pressure has shown that pressure-temperature phase diagram belongs to the type displayed in Figure 1b.<sup>6</sup> This provides evidence for the disappearance of FCC phase at pressures higher than the triple point sharing liquid and R and FCC OD phases (31 MPa, 278.7 K). It should be emphasized that, first, according to the  $p$ – $T$  diagram, the extrapolation of melting curve of the R phase at normal pressure gives the temperature at which R phase would melt if the FCC phase would not exist and, second, that such an extrapolated value falls in the temperature stability domain of OD FCC phase at normal pressure. It is obvious that depending on the thermodynamic properties of the OD phases, which all of them are a consequence of a balance between intermolecular interactions and steric conditions, an additional case, shown in Figure 1c, can appear. In such a case, the topology of the two-phase equilibria generates R–FCC–L and Or–R–FCC triple points (Or, being the low-temperature ordered phase) on the positive pressure domain (Figure 1c). This is in contrast to the previous case (Figure 1b) for which the triple point between the low-temperature ordered phase and the OD phases (FCC and R) falls at negative pressures (as for the  $\text{CBrCl}_3$ ).<sup>6</sup>

The polymorphism of  $\text{CBr}_2\text{Cl}_2$  at normal pressure has been studied by several methods.<sup>3–5</sup>

The crystal structure of the low-temperature ordered form is monoclinic  $C2/c$  with  $Z = 32$  as inferred from neutron powder diffraction.<sup>4</sup> At 259 K, monoclinic phase transforms into an OD phase, the symmetry of which is FCC. The latter phase is stable up to the melting at ca. 294 K.<sup>3</sup>

The crystal structures of the ordered and OD phases of  $\text{CBrCl}_3$  were attempted by Binbrek et al.<sup>4</sup> They described the structure of the phase III of  $\text{CBrCl}_3$ , from neutron powder diffraction, in terms of the  $C2/c$  space group with  $Z = 32$ , on the basis of the hypothesis of the isostructural character with  $\text{CBr}_4$  and  $\text{CCl}_4$ . Thus, as far as the low-temperature ordered phases are concerned, for the three compounds involved in this work,  $\text{CBrCl}_3$ ,  $\text{CBr}_2\text{Cl}_2$ , and  $\text{CCl}_4$ , all of them are isostructural (monoclinic  $C2/c$ ,  $Z = 32$ ). This experimental fact enables the possibility of continuous formation of mixed crystals in such an ordered state.

Because the polymorphic behavior of  $\text{CBr}_2\text{Cl}_2$  at normal pressure does not display the existence of an OD R phase, we have explored the possibility of combining the results obtained for the binary systems sharing pure compounds displaying several of the described topological  $p$ – $T$  phase diagrams to

unravel the physical appearance of the rhombohedral phase, which seems to be a “common” possibility of these kinds of compounds concerning a spatial long-range ordering with orientational disorder.

This work is then mainly concerned with the manifestation of the metastable transitions for two-component systems ( $\text{CCl}_4 + \text{CBr}_2\text{Cl}_2$  and  $\text{CBrCl}_3 + \text{CBr}_2\text{Cl}_2$ ) sharing compounds displaying the phase behavior of the schemes depicted in Figure 1a ( $\text{CCl}_4$ )<sup>35</sup> and 1b ( $\text{CBrCl}_3$ )<sup>6</sup> to contribute to the understanding of the metastable behavior of a possible rhombohedral phase of  $\text{CBr}_2\text{Cl}_2$  at normal pressure by the influence of the stability at high-pressure. The phase behavior of the two systems is examined from the viewpoints of crystallography and thermodynamics. With regard to the thermodynamic analysis a main part is devoted to the phenomenon of crossed isopolymorphism.<sup>23,36</sup> The present paper underlines their importance and at the same time provides new experimental evidence.

To unravel the characteristics of the two-component systems we have then used three strongly complementary techniques, the differential scanning calorimetry, which enables us to characterize the phase transitions of the mixed crystals; the X-ray powder diffraction, which accounts for the lattice properties of each phase as well as assures the one- or two-phase domains in the binary systems; and, finally, the thermodynamic analysis of each particular system, which permits us to coherently rationalize the thermodynamic data, to account for the stability/metastability of the phases and to derive the excess properties of the solid phases.

## 2. Experimental Section

**2.1. Materials.** The chemicals  $\text{CCl}_4$  and  $\text{CBrCl}_3$  were obtained from Across with purity of 99+% and 99%, respectively. They were used as received since the measured melting points agreed well with the ones reported earlier.<sup>3,6</sup>  $\text{CBr}_2\text{Cl}_2$  was obtained from Aldrich and fractionally distilled, the final compound showing a melting temperature which agrees with previous works.

Binary mixtures were prepared at room temperature, i.e., in the liquid state, by mixing the materials in the desired proportions.

**2.2. Thermal Analysis.** A low-temperature equipped Perkin-Elmer DSC-7 differential scanning calorimeter was used to conduct calorimetric measurements, performed with Perkin-Elmer high-pressure stainless-steel pans to prevent reaction with the container. Heating and cooling rates of  $2 \text{ K}\cdot\text{min}^{-1}$  and sample masses around 15 mg were typically used.

**2.3. X-ray Powder Diffraction.** High-resolution X-ray powder diffraction patterns using the Debye–Scherrer geometry and transmission mode were recorded with a horizontally mounted INEL cylindrical position-sensitive detector (CPS-120) made of 4096 channels (angular step ca.  $0.029^\circ(2\theta)$ ).<sup>37</sup> Monochromatic  $\text{Cu K}\alpha_1$  ( $\lambda = 1.54059 \text{ \AA}$ ) radiation was selected by means of an asymmetrically focusing incident beam curved quartz monochromator. The generator power was set to 40 kV and 30 mA. Low-temperature measurements were achieved with a liquid nitrogen 600 series Cryostream Cooler from Oxford Cryosystems.

External calibration using  $\text{Na}_2\text{Ca}_3\text{Al}_2\text{F}_4$  cubic phase was performed to convert channels to  $2\theta$  degrees by means of cubic spline fittings to correct the deviation from angular linearity in PSD<sup>38</sup> and the peak positions were determined by pseudo-Voigt fittings. After indexing the patterns lattice parameters of the OD phases were refined while patterns of the low-temperature ordered phases were submitted to a Rietveld profile refinement

**TABLE 1: Temperatures and Enthalpy and Entropy Changes Associated with the Phase Transitions of  $\text{CCl}_4$ ,  $\text{CBrCl}_3$ , and  $\text{CBr}_2\text{Cl}_2$  Obtained in This Work and from Previously Reported Adiabatic Calorimetry<sup>3,a</sup>**

	transition	T/K	$\Delta H/\text{kJ}\cdot\text{mol}^{-1}$	$\Delta S/\text{J}\cdot\text{mol}^{-1}\cdot\text{K}^{-1}$	reference
$\text{CCl}_4$	$\text{M}^{\text{S}} \rightarrow \text{R}^{\text{S}}$	225.9	4.68	20.72	8
		225.35	4.581	20.33	19
		$225.70 \pm 0.01$	$4.631 \pm 0.020$	20.52	20
	$\text{R}^{\text{S}} \rightarrow \text{L}^{\text{S}}$	250.3	2.52	10.06	8
		250.3	2.515	10.05	19
		$250.53 \pm 0.01$	2.562	10.23	20
		245.8	1.82	7.42	8
	$\text{FCC}^{\text{m}} \rightarrow \text{L}^{\text{m}}$	$246.01 \pm 0.01$	$1.830 \pm 0.070$	7.44	20
	$\text{R}^{\text{m}} \rightarrow \text{FCC}^{\text{m}}$	262.9 <sup>d</sup>	0.69 <sup>d</sup>	2.64 <sup>d</sup>	8
		258.0 <sup>c</sup>	0.66 <sup>c</sup>	257 <sup>c</sup>	40
$\text{CBrCl}_3$	$\text{M}^{\text{S}} \rightarrow \text{R}^{\text{S}}$	238.1	4.58	19.23	8
		238.19	4.618	19.40	3
	$\text{R}^{\text{S}} \rightarrow \text{FCC}^{\text{S}}$	260.3	0.52	1.98	8
		259.34	0.527	2.03	3
	$\text{FCC}^{\text{S}} \rightarrow \text{L}^{\text{S}}$	267.1	2.03	7.61	8
		267.9	2.032	7.59	3
	$\text{R}^{\text{m}} \rightarrow \text{L}^{\text{m}}$	265.7 <sup>c</sup>	2.55 <sup>c</sup>	9.58 <sup>c</sup>	8
		265.5 <sup>c</sup>	2.55 <sup>c</sup>	9.59 <sup>c</sup>	41
		258.8	5.22 <sup>b</sup>	20.19	this work
	$\text{CBr}_2\text{Cl}_2$	$\text{M}^{\text{S}} \rightarrow \text{FCC}^{\text{S}}$	258.8	5.431	21.06
262.0 <sup>c</sup>			4.80 <sup>c</sup>	18.32 <sup>c</sup>	this work
$\text{FCC}^{\text{S}} \rightarrow \text{L}^{\text{S}}$		293.7	2.30	7.82	this work
		294.4	2.308	7.89	3
$\text{R}^{\text{m}} \rightarrow \text{FCC}^{\text{S}}$		243.6 <sup>c</sup>	0.436 <sup>c</sup>	1.79 <sup>c</sup>	this work
		280.7 <sup>c</sup>	2.36 <sup>c</sup>	8.40 <sup>c</sup>	this work

<sup>a</sup> The stable and metastable transitions are denoted by superscripts (s) and (m), respectively. M refers to the low-temperature monoclinic (C2/c) phase of  $\text{CCl}_4$ ,  $\text{CBrCl}_3$ , and  $\text{CBr}_2\text{Cl}_2$ , and R and FCC for the rhombohedral and face-centered cubic OD phases. <sup>b</sup> The small disagreement (<5%) for the  $\Delta H^{\text{M}-\text{FCC}}$  value of this work to that obtained by means adiabatic calorimetry could be ascribed to the addition by the authors of ref 3 of some pretransitional effects appearing at the M to FCC transition as superimposed to the vibrational heat capacity in the monoclinic phase (see Figure 1 of ref 6) <sup>c</sup>Values obtained from the extrapolation of experimental values. <sup>d</sup> Values obtained from fundamental thermodynamics (see text).

by means FullProof program.<sup>39</sup> Details of the procedure are given in Section 3.2.

Liquid samples were placed into 0.3 mm-diameter Lindemann capillaries at room temperature and were rotated perpendicularly to the X-ray beam during data collection to improve averaging of the crystallites. Acquisition times were around 60 min for measurements in the OD phases and no less than 120 min for the low-temperature ordered phases.

### 3. Results

**3.1. Differential Scanning Calorimetry.** The thermodynamic properties of the phase transitions for the pure halogenomethane compounds are given in Table 1. At present only values corresponding to phase changes between phases denoted by the superscript (s), which correspond to the experimental available transitions, should be considered. Such values match quite well with previously reported values.

The reader must pay attention to some evidence, which will be of importance for the following sections describing the two-component systems. Both  $\text{CCl}_4$  and  $\text{CBrCl}_3$  compounds display stable OD phases with rhombohedral symmetry, while the OD FCC phase is stable for  $\text{CBrCl}_3$  and metastable (but experimentally available) for  $\text{CCl}_4$ . The OD stable phase for the compound  $\text{CBr}_2\text{Cl}_2$  has FCC symmetry.

The DSC output was used to establish the complete melting and solid–solid transition temperatures, as well as the concomitant heat effect, both as a function of composition. To determine the stable phase diagram, mixed samples were cooled from room temperature down to at least 180 K at  $2 \text{ K}\cdot\text{min}^{-1}$  and heated back to room temperature. In fact, the information on the systems comes from combining X-ray diffraction as a function of temperature and composition, with differential scanning calorimetry, the former being detailed later.

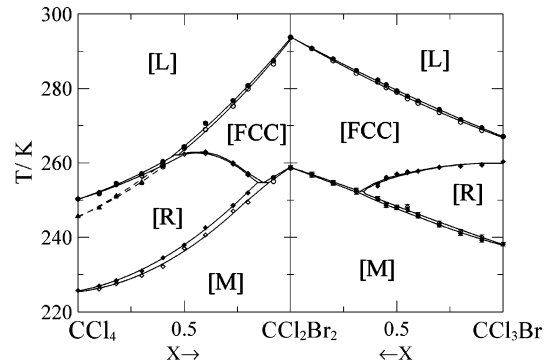


**Figure 2.** Temperature–composition  $\text{CCl}_4 + \text{CBr}_2\text{Cl}_2$  and  $\text{CBrCl}_3 + \text{CBr}_2\text{Cl}_2$  two-component systems showing the stable (continuous line) two-phase equilibria. The metastable part of the [FCC + L] equilibrium for the  $\text{CCl}_4 + \text{CBr}_2\text{Cl}_2$  system is also displayed as a dashed line.

In Figure 2 the characteristic temperatures of the two-phase equilibria are shown as a function of composition for both  $\text{CCl}_4 + \text{CBr}_2\text{Cl}_2$  and  $\text{CBrCl}_3 + \text{CBr}_2\text{Cl}_2$  two-component systems. The results of the enthalpy of the solid–solid-phase transitions and melting obtained for both systems are shown in Figure 3.

Experimental evidence shared by the two-component systems is the existence of continuous OD FCC mixed crystals. It should be noticed that such mixed crystals for the  $(\text{CCl}_4)_{1-X}(\text{CBr}_2\text{Cl}_2)_X$  two-component system can be classified into two different categories: (i) mixed crystals with molar compositions within the  $0.40 < X < 1$  composition range for which the phase transitions appearing upon cooling are liquid to FCC and FCC to R or to M, all of them being reversible and thus evidenced the enantiotropic relation between both OD phases in this composition range, (ii) for mixed crystals with molar composition lower than ca. 0.40, two phase transitions involving OD occur upon cooling while only one occurs upon heating back

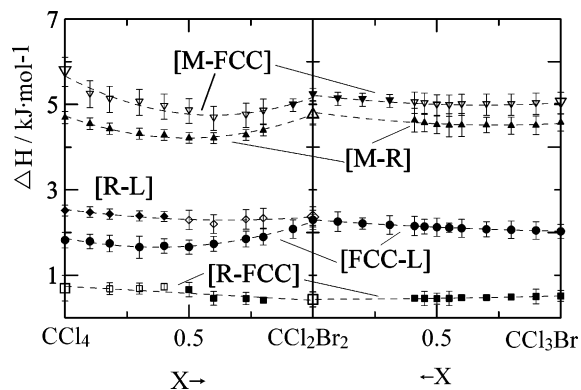


**Figure 3.** Experimental enthalpies (full symbols) of melting of FCC (●) and R (◆) and for the R to FCC (■) and the M to R (▲) or FCC (▼) transitions as a function of the mole fraction. Empty symbols are obtained either by extrapolation of the curves or by eq 1 (see text).

to room temperature. The sequence upon cooling (as revealed by X-ray diffraction measurements) is related to the liquid-FCC and FCC-R phase transitions. The R mixed crystals do not revert to the FCC phase upon heating back and only melting of the R phase is found. When cooling is limited such the FCC phase is formed, this phase melts upon heating without transformation to the R phase, as it occurs for the  $\text{CCl}_4$  pure compound. Thus, the same monotropic behavior between R and FCC phases is found for that composition range of mixed crystals.

As far as mixed samples of the  $\text{CBrCl}_3 + \text{CBr}_2\text{Cl}_2$  system are concerned, it appears that the FCC mixed crystals are stable for the whole range of composition.

Another relevant fact (as we will demonstrate in the crystallographic section) is the existence of continuous formation of low-temperature monoclinic mixed crystals whatever the system. This makes evident the isomorphism relation between the low-temperature ordered phases of all the compounds involved in this work and, confirms the results obtained by Binbrek et al.,<sup>4</sup> who determined the structure of  $\text{CBr}_2\text{Cl}_2$  in terms of the  $C2/c$  space group by postulating that all the members of the  $\text{CBr}_n\text{Cl}_{4-n}$  ( $n = 0, \dots, 4$ ) were isostructural and assuming that the molecules are disordered so that sites have equivalent fractional occupancies for chlorine and bromine atoms.

According to the described thermal analysis measurements, the enthalpy changes associated with the melting of the FCC mixed crystals were measured continuously for the whole composition range in both binary systems (Figure 3). As far as the melting of the R mixed crystals is concerned, direct information is only obtained from the  $\text{CCl}_4 + \text{CBr}_2\text{Cl}_2$  system for the  $0 < X < 0.40$  composition range. In spite of such a limited availability, the complete variation of the melting enthalpy of R mixed crystals can be obtained by adding the heat of the R to FCC transition to the melting of the FCC mixed crystals. Such a calculation is based on the following equation:

$$\Delta H_{\phi \rightarrow \gamma} = \Delta H_{\phi \rightarrow \alpha} + \Delta H_{\alpha \rightarrow \gamma} \quad (1)$$

applied for  $\phi \equiv \text{R}$ ,  $\gamma \equiv \text{L}$  and  $\alpha \equiv \text{FCC}$ . This equation assumes that the specific heats of both  $\phi$  and  $\alpha$  phases are close, as is the case for both OD FCC and R phases. In this way, extrapolation at  $X = 1$  of the melting enthalpy change of the R mixed crystals provides the heat effect associated with the melting of a virtual R (metastable) phase of the  $\text{CBr}_2\text{Cl}_2$  compound. The obtained value is  $\Delta_{\text{R}}^{\text{L}}H = (2.36 \pm 0.15)\text{kJ}\cdot\text{mol}^{-1}$ .

To end this section, we would like to point out that the extrapolation of the [R + FCC] two-phase equilibrium as well as the associated enthalpy change at  $X = 1$  ( $\text{CBr}_2\text{Cl}_2$ ) enables

us to infer the characteristic values of a virtual transition between a metastable R phase to the stable FCC phase for the  $\text{CBr}_2\text{Cl}_2$  compound ( $T^{\text{R-FCC}} = 243.6 \pm 2.0 \text{ K}$  and  $\Delta_{\text{R}}^{\text{FCC}}H = (0.436 \pm 0.080)\text{kJ}\cdot\text{mol}^{-1}$ ). Such value can be physically interpreted as the extrapolation at normal pressure of a high-pressure two-phase equilibrium between R and FCC phases as indicated in Figure 1c. It should be noticed that the  $T^{\text{R-FCC}}$  value falls into the temperature stability domain of the low-temperature ordered (monoclinic) phase ruling out the pressure-temperature diagram displayed in Figure 1d. It is also noteworthy that with increasing mole fraction of the [R + L] melting equilibrium of the  $\text{CCl}_4 + \text{CBr}_2\text{Cl}_2$  system would end (at  $X = 1$ ) at the non-experimentally available melting temperature of phase R of  $\text{CBr}_2\text{Cl}_2$ ,  $T^{\text{R-L}}$ . Finally, with the same coherence as for the previous transitions, a M to R solid–solid transition ( $T^{\text{M-R}}$ ) appears for the  $\text{CBr}_2\text{Cl}_2$  compound.

**3.2. Crystallographic Characterization.** The isomorphism relationships between the isostructural phases have been shown by determining the continuity of the lattice parameters as a function of composition by means of X-ray powder diffraction studies at different temperatures.

**3.3. Monoclinic Mixed Crystals.** X-ray powder diffraction measurements were undertaken at 220.2 K for the monoclinic ( $C2/c$ ,  $Z = 32$ ) mixed crystals in both two-component systems for several compositions. To carry out the analysis of the X-ray patterns of these “ordered” mixed crystals, we have performed a Rietveld profile refinement by means of Fullprof software.<sup>39</sup> The process was successfully followed for the  $\text{CCl}_4 + \text{CBrCl}_3$  mixed crystals in a previous work<sup>8</sup> and consists mainly on the procedure described by Binbrek et al. for pure compounds  $\text{CBrCl}_3$  and  $\text{CBr}_2\text{Cl}_2$ .<sup>4</sup> As the starting configurations we used the atomic coordinates of the four molecules in the asymmetric unit of  $\text{CCl}_4$  or  $\text{CBrCl}_3$  (for the  $\text{CCl}_4 + \text{CBr}_2\text{Cl}_2$  and  $\text{CBrCl}_3 + \text{CBr}_2\text{Cl}_2$  mixed crystals, respectively). Fractional occupancies of the halogen sites were set according to the composition of the analyzed mixed crystal and molecules were represented by a rigid body with tetrahedral symmetry. Varying slightly the fractional occupancies around the values of the exact composition determined by the chlorine and bromine atoms participating in the mixed crystal did not result in a substantial decreasing of the related R-factors, precluding then a partial “ordering” of the mixed crystals in regard to the halogen disorder described for pure compounds.<sup>4,8</sup> Two representative examples of the experimental and calculated profiles for two mixed crystals  $(\text{CCl}_4)_{0.51}(\text{CBr}_2\text{Cl}_2)_{0.49}$  and  $(\text{CBrCl}_3)_{0.55}(\text{CBr}_2\text{Cl}_2)_{0.45}$  are given in Figure 4 together with that of the  $\text{CBr}_2\text{Cl}_2$  pure compound.

Following the same procedure for several mixed crystals with molar fractions distributed along the whole concentration range, the lattice parameters vs concentration were determined and are shown in Figure 5. The continuous variation of the lattice parameters with concentration establishes the existence of an isomorphism relationship between the low-temperature ordered phases of the three pure compounds involved, confirming the structural results found for  $\text{CBrCl}_3$  and  $\text{CBr}_2\text{Cl}_2$  from neutron powder diffraction on the hypothesis that both compounds were isostructural to  $\text{CCl}_4$  and  $\text{CBr}_4$ . It is to be noticed that lattice parameters of both series of mixed crystals nicely converge at the same values for  $X = 1$ , i.e., the  $\text{CBr}_2\text{Cl}_2$  pure compound. In addition, monoclinic lattice parameters of  $\text{CBr}_2\text{Cl}_2$  determined at 220.2 K ( $a = 20.872(4) \text{ \AA}$ ,  $b = 11.747(2) \text{ \AA}$ ,  $c = 20.434(4) \text{ \AA}$ ,  $\beta = 111.19(1)^\circ$ ,  $V/Z = 146.0 \text{ \AA}^3$ ) agree quite well with those previously published.<sup>4</sup>

**3.4. OD Mixed Crystals.** **3.4.1. Face-Centered Cubic Mixed Crystals.** From previous DSC experiments, the concentration

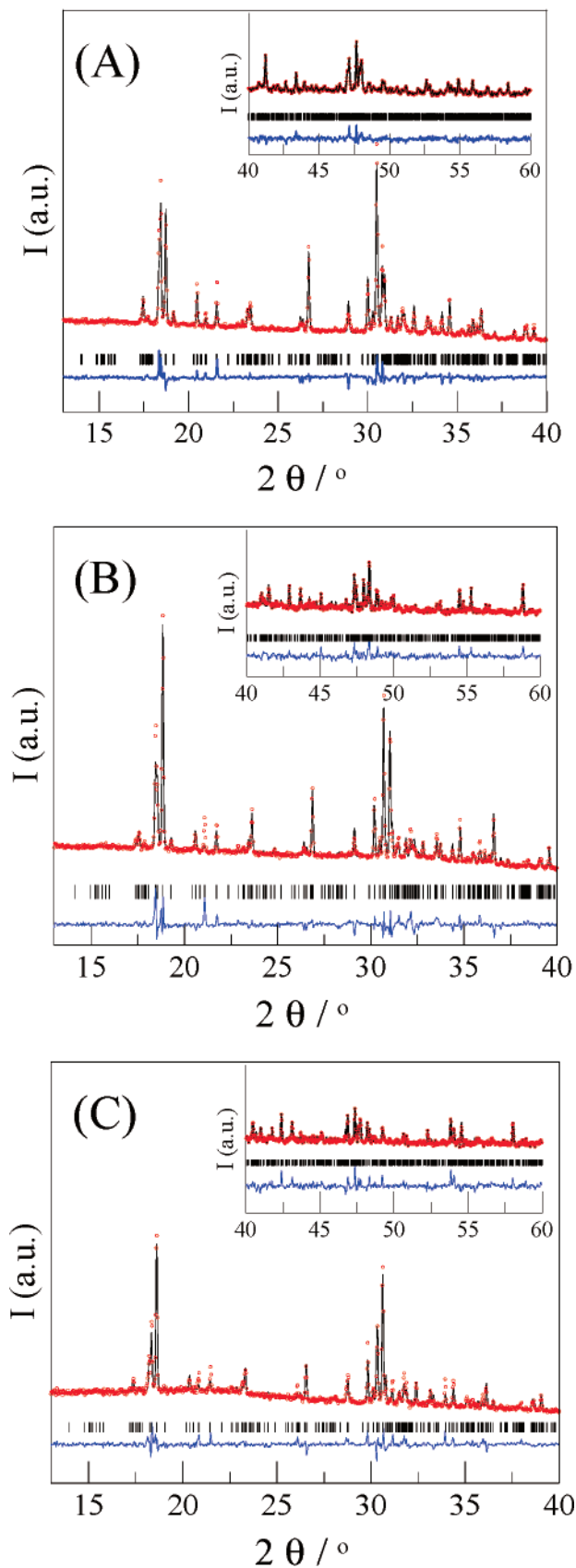


**Figure 4.** Experimental (o) and theoretical (black line) diffraction patterns along with the difference profile of monoclinic phase at 220.2 K (blue line at the bottom of each panel) for (A)  $\text{CBr}_2\text{Cl}_2$  pure compound ( $R_p = 7.08\%$ ,  $R_{wp} = 9.88\%$ ) and (B)  $(\text{CCl}_4)_{0.51}(\text{CBr}_2\text{Cl}_2)_{0.49}$  ( $R_p = 5.32\%$ ,  $R_{wp} = 7.42\%$ ) and (C)  $(\text{CBrCl}_3)_{0.55}(\text{CBr}_2\text{Cl}_2)_{0.45}$  ( $R_p = 5.30\%$ ,  $R_{wp} = 7.23\%$ ) mixed crystals. Each inset corresponds to a five times expanded vertical scale for the 40–60°  $2\theta$ -range.

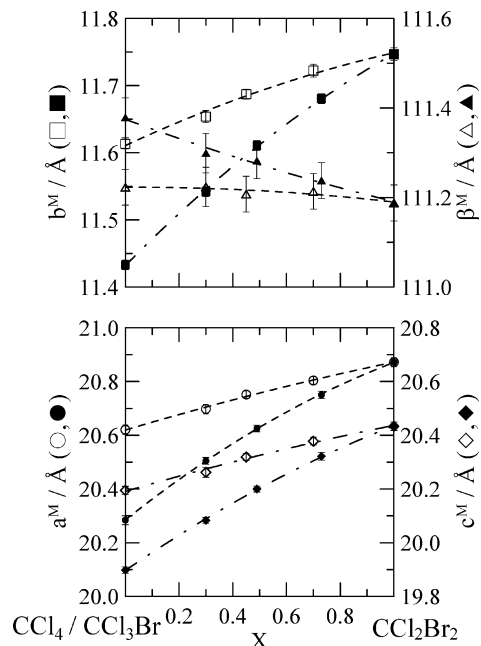


**Figure 5.** Lattice parameters as a function of the mole fraction for the low-temperature monoclinic mixed crystals at 220.2 K of the  $\text{CCl}_4 + \text{CBr}_2\text{Cl}_2$  (full symbols) and  $\text{CBrCl}_3 + \text{CBr}_2\text{Cl}_2$  (empty symbols) two-component systems.

ranges for the enantiotropic or monotropic behavior as well as the limit of metastability for which FCC mixed crystals obtained by cooling from the liquid were clearly stated for the  $\text{CCl}_4 + \text{CBr}_2\text{Cl}_2$  system. Such a procedure enabled to measure at 241.2 K for the whole concentration range the variation of the lattice parameter vs mole fraction in the aforementioned system, with the exception of the pure compound  $\text{CBr}_2\text{Cl}_2$  for which the quoted value was obtained by extrapolation of the cubic parameter as a function of temperature. As for the  $\text{CBrCl}_3 + \text{CBr}_2\text{Cl}_2$  system, the OD FCC mixed crystals display a complete stable domain as regard to the composition, so they were crystallographically characterized in that region at 265.2 K.

The results for both systems are shown in Figure 6. The continuity of both curves demonstrates the isomorphism relationship between the monotropic FCC of  $\text{CCl}_4$  and the enantiotropic FCC phases of  $\text{CBr}_2\text{Cl}_2$  and  $\text{CBrCl}_3$ .

**3.4.2. Rhombohedral Mixed Crystals.** In this case, Lindemann capillaries were cooled down to the stable low-temperature monoclinic phase and heated again up to the temperature at which the measurements were carried out. This path ensures that stable R mixed crystals are formed. Figure 6 shows the variation of the R lattice parameters as a function of the mole fraction at 243.2 and 253.2 K for the  $\text{CCl}_4 + \text{CBr}_2\text{Cl}_2$  and  $\text{CBrCl}_3 + \text{CBr}_2\text{Cl}_2$  systems, respectively. By assuming the existence of a metastable R phase for  $\text{CBr}_2\text{Cl}_2$  compound, it can be inferred that a “virtual” continuous series of mixed crystals in the R phase would give rise to an isomorphism relationship. The lattice parameters for that metastable R phase of  $\text{CBr}_2\text{Cl}_2$  compound can be obtained with more accuracy at 243.2 K from the extrapolation performed in the  $\text{CCl}_4 + \text{CBr}_2\text{Cl}_2$  system ( $a^R(243.2 \text{ K}) = 14.772(15) \text{ \AA}$ ,  $\alpha^R(243.2 \text{ K}) = 89.44(2)^\circ$ ).

**3.5. Thermodynamic Analysis Procedure.** The purpose in this section is to bring together the experimental data of both systems and to subject them to a thermodynamic analysis. Next, we explore the possibility of combining the results obtained for each individual system to a coherent and unifying descrip-

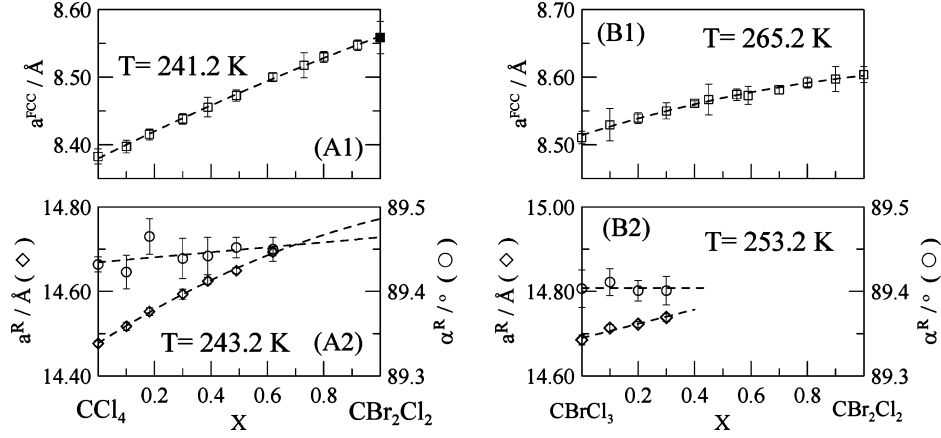


**Figure 6.** Lattice parameters as a function of the mole fraction for the OD FCC (A1 and B1) and R (A2 and B2) mixed crystals. Temperature at which they were measured is detailed inside each panel. Full square for the FCC lattice parameter  $a$  at 241.2 K comes from the extrapolation of the lattice parameter variation with temperature for the pure compound  $\text{CBr}_2\text{Cl}_2$ .

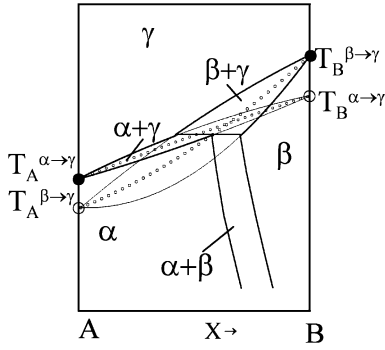


**Figure 7.** Solid and dashed curves represent stable and metastable behavior, respectively. Full and open circles represent the stable and metastable transition points, respectively. The small-circle lines represent the EGC-curves.

tion, in particular with regard to the inference of thermodynamic properties of a virtual R phase of  $\text{CBr}_2\text{Cl}_2$  compound.

**3.5.1. Thermodynamic Formulation.** We have reported in detail on the thermodynamic formalism we use in other works.<sup>8,23–25</sup> Here, we repeat only the pertinent information for the sake of completeness. To follow the used thermodynamic analysis procedure, it is expedient then to describe the case referred to as crossed isopolymorphism<sup>23,36</sup> sketched in Figure 7. The form  $\alpha$  is stable for component A, while the form  $\beta$  is stable for component B ( $\beta$  is metastable for A and  $\alpha$  is metastable for B),  $\gamma$  being stable for both components. The “stable” phase diagram can be looked upon as the stable result of two crossing two-phase loops. The two crossing loops imply a stable three-phase equilibrium ( $\alpha + \beta + \gamma$ ), which, in the case of Figure 7, is peritectic.

Any phase  $\phi$  we consider in which  $(1 - X)$  mole of component A mixes with  $X$  mole of component B, is characterized by its own Gibbs function

$$G^\phi(T, X) = (1 - X)\mu_A^{*\phi}(T) + X\mu_B^{*\phi}(T) + RT[X \ln(X) + (1 - X)\ln(1 - X)] + G^{E,\phi}(T, X) \quad (2)$$

where  $T$  stands for the thermodynamic temperature,  $R$  the gas constant,  $\mu_k^{*\phi}(T)$ ,  $k = A, B$  denote the molar Gibbs energies of the components, and  $G^{E,\phi}(T, X)$  denotes the excess Gibbs energy which accounts for the deviation of the mixture in the  $\phi$  phase from ideal-mixing behavior produced by interactions between molecular species A and B with regard to the interactions between molecules of the same species (A–A and B–B).

To determine the two-phase equilibrium region between two phases ( $\phi$  and  $\gamma$ ), i.e., the concentration limits of the loop for the coexisting phases, the well-known equilibrium rule minimizing the Gibbs energy of the mixed crystal  $A_{1-X}B_X$  at each temperature, which consists on the common tangent to both Gibbs energies characterizing the phases of the corresponding equilibrium,  $G^\phi(T, X)$  and  $G^\gamma(T, X)$ , must be determined. For this task, the molar Gibbs energies of the pure compounds A and B as well as the excess properties for each phase are required. Because of the lack of data on  $\mu_k^{*\phi}$ ,  $k = A, B$  and  $\phi = \alpha, \beta, \gamma$  the simplified treatment of the equal-Gibbs curve-(EGC-) method will be used.<sup>42</sup>

To do so, the difference between the Gibbs energies of phases  $\phi$  and  $\gamma$  is written as

$$\Delta_\phi^\gamma G(T, X) = G^\gamma(T, X) - G^\phi(T, X) = (1 - X)\Delta_\phi^\gamma \mu_A^*(T) + X\Delta_\phi^\gamma \mu_B^*(T) + \Delta_\phi^\gamma G^E(T, X) \quad (3)$$

where  $\Delta_\phi^\gamma \mu_k^*(T)$  is  $\mu_k^{*\gamma} - \mu_k^{*\phi}$  ( $k = A, B$ ) and  $\Delta_\phi^\gamma G^E(T, X)$  is the excess Gibbs energy difference between the considered phases, i.e.,  $G^{E,\gamma}(T, X) - G^{E,\phi}(T, X)$ .

Because the existence of equilibrium at a given temperature necessarily implies that the Gibbs functions of the  $\phi$  and  $\gamma$  phases intersect, it follows that the locus of the points of intersection in the  $TX$  plane (the EGC) will be the result of this equation:

$$\Delta_\phi^\gamma G(T_{\text{EGC}}, X) = 0 \quad (4)$$

By neglecting the heat capacities differences between both phases,  $\Delta_\phi^\gamma \mu_k^*(T)$  can be approximately written as  $\Delta_\phi^\gamma S_k^*(T_k^{\phi \rightarrow \gamma} - T)$ , being  $T_k^{\phi \rightarrow \gamma}$  the temperature of the  $\phi \rightarrow \gamma$  transition for the component  $k$ , the EGC temperature can be deduced from eq 4 as shown:

$$T_{\text{EGC}} = \frac{(1 - X)\Delta_\phi^\gamma H_A^* + X\Delta_\phi^\gamma H_B^*}{(1 - X)\Delta_\phi^\gamma S_A^* + X\Delta_\phi^\gamma S_B^*} + \frac{\Delta_\phi^\gamma G_{\text{EGC}}^E(X)}{(1 - X)\Delta_\phi^\gamma S_A^* + X\Delta_\phi^\gamma S_B^*} \quad (5)$$

where  $\Delta_\phi^\gamma H_k^*$  and  $\Delta_\phi^\gamma S_k^*$  are the enthalpy and entropy changes of the  $\phi \rightarrow \gamma$  transition for the component  $k$ . The first term of the right side of eq 5 represents the EGC temperature for the  $[\phi + \gamma]$  equilibrium when the excess Gibbs energy difference is zero and is only pure component-dependent and thus can be obtained from pure component data. Nevertheless, some of the metastable

**TABLE 2:**  $\Delta_{\alpha}^{\beta}G_1 = G_1^{\beta} - G_1^{\alpha}$  and  $\Delta_{\alpha}^{\beta}G_2 = G_2^{\beta} - G_2^{\alpha}$  Parameters of the Redlich–Kister Polynomial for the Excess Gibbs Energy Difference between the Involved Phases in the  $\text{CCl}_4 + \text{CBr}_2\text{Cl}_2$  and  $\text{CBr}_2\text{Cl}_2 + \text{CBrCl}_3$  Two-Component Systems Together with the Equimolar Equal-Gibbs Temperature ( $T_{\text{EGC}}(X = 0.5)$ ) for Each of the Assessed Equilibria

equilibrium	$\alpha$	$\beta$	$\text{CCl}_4 + \text{CBr}_2\text{Cl}_2$			$\text{CBr}_2\text{Cl}_2 + \text{CBrCl}_3$		
			$\Delta_{\alpha}^{\beta}G_1 \text{ J}\cdot\text{mol}^{-1}$	$\Delta_{\alpha}^{\beta}G_2 \text{ J}\cdot\text{mol}^{-1}$	$T_{\text{EGC}}(X = 0.5) \text{ K}$	$\Delta_{\alpha}^{\beta}G_1 \text{ J}\cdot\text{mol}^{-1}$	$\Delta_{\alpha}^{\beta}G_2 \text{ J}\cdot\text{mol}^{-1}$	$T_{\text{EGC}}(X = 0.5) \text{ K}$
[FCC + L]	FCC	L	-149	-37	264.7	-44	-27	279.2
[R + L]	R	L	-85	-95	262.9	-13 <sup>a</sup>	-13 <sup>a</sup>	-
[R + FCC]	R	FCC	64	-59	262.4	32	14	256.5
[M + FCC]	M	FCC	-254	-253	240.6	-18	-41	248.8
[M + R]	M	R	-318	-177	238.6	-49	-55	248.7

<sup>a</sup> The [R + L] equilibrium does not make a physical appearance in the  $\text{CBr}_2\text{Cl}_2 + \text{CBrCl}_3$  two-component system, but excess Gibbs energy difference is given for completeness.

properties as heats of transition and transition points have to be obtained in an indirect manner when a crossed-isomorphism is considered.

A first estimation of the EGC curve can be done from the experimental data of the two-phase equilibrium. An iterative procedure performed by means of the WINIFIT program<sup>43</sup> based on Onk’s method and on the well-known LIQFIT program<sup>44</sup> enables one to obtain reasonable values of the excess Gibbs energy differences at the EGC temperature by means of eq 5. More details on the computational procedure can be found in ref 45. Because of the lack of the thermodynamic excess properties of the liquid phase, only excess Gibbs energy differences ( $\Delta_{\phi}^{\gamma}G^{\text{E}}$ ) have been determined.

In this framework, the description of the excess Gibbs energy difference was given by a two-parameter function in the form of a Redlich–Kister polynomial

$$\Delta_{\phi}^{\gamma}G^{\text{E}}(X) = X(1 - X)[\Delta_{\phi}^{\gamma}G_1 + \Delta_{\phi}^{\gamma}G_2(1 - 2X)] \quad (6)$$

which in the lack of strong local anomalies is fairly adequate and physically understandable:  $\Delta_{\phi}^{\gamma}G_1$  expresses the magnitude of the excess Gibbs energy difference at the equimolar composition and  $\Delta_{\phi}^{\gamma}G_2$ , gives account for the asymmetry of such a function with respect to  $X = 0.5$ . In addition, we consider the  $\Delta_{\phi}^{\gamma}G_1$  and  $\Delta_{\phi}^{\gamma}G_2$  coefficients to be temperature-independent due to the small range of temperature in which two-phase equilibria exists.

**3.5.2. The Simple [FCC + L] Two-Phase Equilibria.** In the case of the two-component systems analyzed here, the  $\text{CBr}_2\text{Cl}_2$  component displays a stable OD FCC phase, which according to the calorimetric and crystallographic characterization is isomorphous to the metastable OD FCC phase of  $\text{CCl}_4$  and to the stable OD FCC phase of  $\text{CBrCl}_3$ .

The temperatures and enthalpy changes corresponding to the FCC melting of the pure compounds (see Table 1), all of them experimentally available, and the temperature data of the equilibrium were used for the thermodynamic assessment. It results in the excess Gibbs energy differences expressed by the Redlich–Kister coefficients given in Table 2.

**3.5.3. Crossed Isopolymorphism: [R + FCC], [M + R] and [M + FCC] Two-Phase Equilibria.** As for the equilibria involving R, FCC and M phases, the nonexistence of an OD R phase for the  $\text{CBr}_2\text{Cl}_2$  compound forces to an estimation of the thermodynamic properties of a such virtual phase (isomorphous to the R phase of both  $\text{CCl}_4$  and  $\text{CBrCl}_3$  compounds) for that compound. Such an estimation is performed by the metastable extensions of the [R + FCC] loops which ends (at  $X = 1$ ) in the theoretical metastable R to FCC transition point of the pure  $\text{CBr}_2\text{Cl}_2$ . Such estimation is nicely performed simultaneously for the two systems. As can be seen in Figure 8, extrapolations of the [R + FCC] loops converge into the same virtual

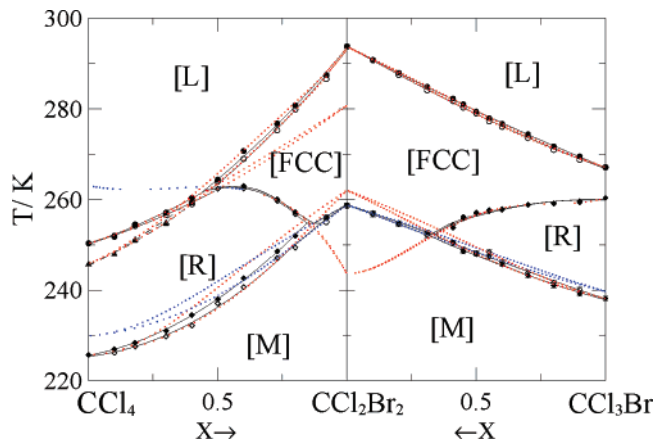


**Figure 8.** Calculated equilibria (red and blue dotted lines), experimental points and stable equilibria (black line).

temperature ( $T_{\text{CBr}_2\text{Cl}_2}^{\text{R-FCC}} = 243.6 \pm 2.0 \text{ K}$ ). As far as the associated enthalpy change  $\Delta_{\text{R}}^{\text{FCC}}H$ , extrapolation of the values for the R to FCC phase transition (see Figure 3), some of them being calculated from eq 1, provides, within the experimental error, a virtually equal value for both systems ( $\Delta_{\text{R}}^{\text{FCC}}H = 0.436 \pm 0.080 \text{ kJ}\cdot\text{mol}^{-1}$ ).

It should be mentioned here that the R to FCC transition for the pure  $\text{CCl}_4$  it is not experimentally available. Owing to the monotropic character of the FCC phase with respect to the R phase, such a transition would appear in the stability domain of the liquid phase. The properties of such transition were determined in some previous works<sup>8,40</sup> and thus, details of the procedure to determine the temperature as well as the enthalpy change will be omitted here. Values are listed in Table 1.

The next step in the thermodynamic assessment of the two-component systems consisted on the evaluation of the required data for the analysis of the [M + R] equilibria. Experimental phase diagrams (Figure 2) make evident that composition extension of such equilibria are large enough to determine the temperature for the virtual M to R phase transition for the pure component  $\text{CBr}_2\text{Cl}_2$  ( $T_{\text{CBr}_2\text{Cl}_2}^{\text{M-R}} = 262.0 \pm 2.0 \text{ K}$ ). Figure 3 provides directly the associated enthalpy change ( $\Delta_{\text{M}}^{\text{R}}H = 4.80 \pm 0.18 \text{ kJ}\cdot\text{mol}^{-1}$ ).

With the temperature and enthalpy change calculated values together with the experimental solvus temperatures, the [R + FCC] and [M + R] phase equilibria were computed by using the crossed isodimorphism procedure.

As for the [M + FCC] equilibria, their relevance on the thermodynamic assessment is smaller than the previous ones. Thus properties of the virtual phase transitions as M to FCC for  $\text{CCl}_4$  and  $\text{CBrCl}_3$  were estimated according to the state function character of the enthalpy and entropy magnitudes. Once the described equilibria were calculated and the excess Gibbs

**TABLE 3: Calculated Temperatures and Mole Fractions Characterizing the Three-Phase Equilibria for the Two-Component Systems  $\text{CCl}_4 + \text{CBr}_2\text{Cl}_2$  and  $\text{CBrCl}_3 + \text{CBr}_2\text{Cl}_2$**

invariant		$\text{CCl}_4 + \text{CBr}_2\text{Cl}_2$	$\text{CBrCl}_3 + \text{CBr}_2\text{Cl}_2$
eutectoid [M + R + FCC]	T/K	264.6	252.5
	$X_M$	0.844	0.652
	$X_N$	0.898	0.704
	$X_P$	0.851	0.659
peritectic [R + FCC + L]	T/K	262.5	
	$X_M$	0.434	
	$X_N$	0.479	
	$X_P$	0.477	

energy differences between the involved phases determined, straightforward calculations were performed for the additional equilibria appearing in both phase diagrams. The obtained excess Gibbs energy differences in the form of Redlich–Kister polynomial coefficients are compiled in Table 2.

It should be noticed that an individual experimental temperature point may deviate from the mean trend to a maximum of about 1 K for the melting and [R + FCC] equilibria while and no more than about 2 K for the equilibria involving the low-temperature monoclinic phase.

Another observation that can be made is related to the existence of a maximum and a minimum in the [R + FCC] two-phase equilibrium of the  $\text{CCl}_4 + \text{CBr}_2\text{Cl}_2$  system. In the field of molecular materials, phase diagrams with a maximum are unusual although they seem to appear when chlorine or bromine atoms and methyl groups are combined.<sup>40,46</sup> The closely related two-component system  $\text{CCl}_4 + (\text{CH}_3)_3\text{CBr}$  shows also a [R + FCC] two-phase equilibrium with a minimum and a maximum.<sup>40</sup> As it can be seen from Figure 8, and taking into account all the thermodynamic properties for the transitions between the M, R, FCC, and L phases, a simple calculation provides the properties for the melting of the R phase of  $\text{CBr}_2\text{Cl}_2$ . Values are presented in Table 1.

The complete phase diagrams resulting from the described thermodynamic assessment together with the experimental values are shown in Figure 8. This figure includes also the metastable parts of the loops. The comparison of calculated and experimental results provides us with reassurance about the robustness of the procedures here employed since the former is shown to account for most of the subtleties brought in by the details of the experimental equilibria. Particularly noteworthy is the evidence for the common inferred metastable temperatures by means of the extrapolation of the two-phase equilibria. Thus, in particular, experimentally “hidden” transitions for  $\text{CBr}_2\text{Cl}_2$  compound emerge and their fundamental properties (temperature and enthalpy change) are obtained.

The temperature and the mole fractions of the peritectic and eutectic invariants characterizing the three-phase equilibria are compiled in Table 3 for both systems.

#### 4. Discussion

According to the described polymorphism of the materials involved in the two-component systems, it is straightforwardly seen that OD mixed crystals between the compounds showing, at normal pressure, a monotropic phase ( $\text{CCl}_4$ ) or showing exclusively enantiotropic phases ( $\text{CBrCl}_3$  and  $\text{CBr}_2\text{Cl}_2$ ) can be of two types, either R or FCC. It necessary appears then that a two-phase region (demixing region) between both OD phases will be present in the phase diagrams. Once Rudman et al.<sup>7</sup> proved the rhombohedral lattice symmetry for the stable OD phase of  $\text{CCl}_4$ , the same molecular arrangement was found for

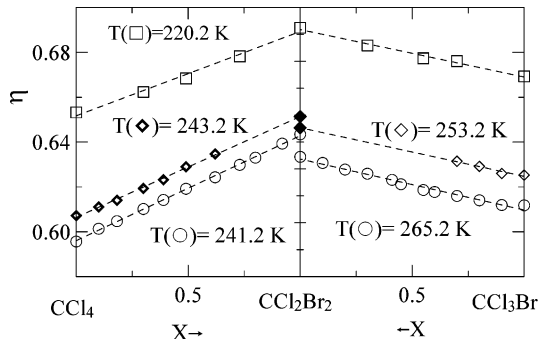


**Figure 9.** Packing coefficient of the monoclinic (squares), rhombohedral (diamonds), and face-centered cubic (circles), mixed crystals. Full diamonds correspond to extrapolated values.

several related methylchloromethane compounds ( $(\text{CH}_3)_{4-n}\text{CCl}_n$ ), at normal pressure ( $n = 2, 3, 4$ )<sup>11,18,20,47</sup> or at high pressure ( $n = 1$ ).<sup>33,34</sup> Recently, such lattice symmetry was disclosed for  $\text{CBrCl}_3$  halogenomethane at normal pressure<sup>6,8</sup> and, the present work proves that a rhombohedral phase makes its (metastable) appearance also for  $\text{CBr}_2\text{Cl}_2$  material. How the rhombohedral phase would be placed on the pressure-temperature phase diagram can be looked upon as sketched in Figure 1c and by “ordering” the phase transition temperatures obtained for  $\text{CBr}_2\text{Cl}_2$  (Table 1): By considering the equivalence of symbols in Figure 1c,  $\alpha = \text{FCC}$ ,  $\beta = \text{R}$ , and  $\text{Or} = \text{M}$ , the temperatures of the stable and metastable phase transitions order as  $T_S^{\text{FCC-L}} > T_m^{\text{R-L}} > T_m^{\text{M-R}} > T_S^{\text{M-FCC}} > T_m^{\text{R-FCC}}$ , which are in perfect agreement with the obtained values ( $293.7 > 280.7 > 262.0 > 258.8 > 243.6$  K). Then, the stability hierarchy of the OD phases and the thermodynamic conditions of their existence can be determined through a topological representation without regarding the details of the specific values for locating triple points.

As far as crystallographic properties of the inferred rhombohedral phase of  $\text{CBr}_2\text{Cl}_2$  are concerned, coherence should be also found. Figure 9 shows the packing coefficient for the ordered and OD mixed crystals. This coefficient is defined as  $\eta = V_m/(V/Z)$ , where  $V_m$  is the molecular volume and  $V/Z$  is the unit-cell volume ( $V$ ) divided by the number of the molecules ( $Z$ ) in the unit cell. As usual, molecular volumes of the pure compounds were calculated using van der Waals radii and interatomic chemical bonds according to the Kitaigorodsky’s method.<sup>48</sup> Values following such procedure are 87.72, 94.29, and 100.86  $\text{\AA}^3$  for  $\text{CCl}_4$ ,  $\text{CBrCl}_3$ , and  $\text{CBr}_2\text{Cl}_2$ , respectively. The packing of the mixed crystals was determined by means of the simplest way, i.e., by setting for a mixed crystal of molar composition  $X$  a linear contribution of the molecular volumes of the A and B molecules shared in the mixed crystal,  $V_m(X) = (1 - X)V_m(\text{A}) + XV_m(\text{B})$ . As expected, the highest packing coefficient corresponds to the low-temperature monoclinic phase (for which strongest interactions and thus greatest density appear). In addition, whatever the degree of stability at normal pressure, the packing of the OD R phase for pure compounds as well as for mixed crystals is higher than that of the OD FCC taking into account the temperature at which values have been determined. Thus, coherent packing coefficient values for the R phase of  $\text{CBr}_2\text{Cl}_2$  are obtained from the extrapolation of OD R mixed crystals in both two-component systems.

Upon increasing mole fraction of  $\text{CBr}_2\text{Cl}_2$ , whatever the phase and whatever the mixed crystals are, packing coefficient increases. Such effect cannot, a priori, be related to either the existence of the R phase at high-pressure nor to the dipole moment of the  $\text{CBr}_2\text{Cl}_2$  molecule, which is virtually the same as for  $\text{CBrCl}_3$  molecule ( $\approx 0.2$  D). In a robust way the evidence

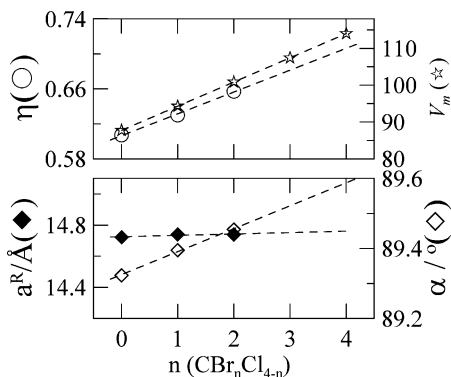


**Figure 10.** Packing and lattice parameter of the rhombohedral phase as a function of the number  $n$  of Bromine atoms for the halogenomethane  $\text{CBr}_n\text{Cl}_{4-n}$  series. Normalized slopes: Packing:  $1/(\eta(n=0))(\partial\eta/\partial n) = 0.041$ ; molecular volume:  $1/(V_m(n=0))(\partial V_m/\partial n) = 0.073$ .

of the coherence of the extrapolated crystallographic properties of the OD R phase of  $\text{CBr}_2\text{Cl}_2$  is shown in Figure 10, corresponding to the OD R lattice parameter and packing coefficient for the halogenomethane compounds for which such phase exists. From that figure noteworthy is the possibility of an OD R phase for compounds  $\text{CBr}_3\text{Cl}$  and  $\text{CBr}_4$ . Thus, although for the first one there is not available information in the literature (synthesis of this compound seems to be difficult),<sup>3,49</sup> for the tetrabromomethane, it has been well established the cubic symmetry of the OD phase at normal pressure, but a high-pressure OD phase has been reported.<sup>50</sup> The existence of high-pressure OD R phases for several members of the family goes along with the normalized slopes of the packing coefficient ( $1/\eta(n=0)(\partial\eta/\partial n) = 0.041$ ) and molecular volume ( $1/V_m(n=0)(\partial V_m/\partial n) = 0.073$ ) as a function of  $n$ : They indicate that unit-cell volume as a function of  $n$  increases slower than molecular volume and thus, the highest packing for high  $n$  values will be compatible with high-pressure phases. For both,  $\text{CBr}_2\text{Cl}_2$  and  $\text{CBr}_4$  high-pressure neutron scattering measurements will be done to determine the coherence of the correlation disclosed by Figure 10.

Molecular dynamic studies of the liquid state for the methylchloromethane compounds ( $(\text{CH}_3)_{4-n}\text{CCl}_n$ ),<sup>26,27</sup> have shown some peculiarities which make difficult to rationalize the net effect of the dipole moment and the polarization. In particular, electrostatic energy for those compounds shows a very low contribution vs nonelectrostatic contribution. In fact, it has been found that in the liquid-state, polarizability for nonpolar molecules (as  $\text{C}(\text{CH}_3)_4$  and  $\text{CCl}_4$ ) has no effect on the structural properties in spite that polarizability are about a factor 7 higher than that of the water. Then, induction effects coming from charge flow within the molecule have been shown to give rise to substantial induced dipole moments for polar molecules.<sup>26</sup> A different work describing the thermodynamic excess properties of the OD mixed crystals between methylchloromethanes, has also revealed the role of the polarizability, which is there called “dipole dilution effect”.<sup>31</sup> When a mixed crystal is formed between a molecule displaying dipolar moment and a molecule devoid of permanent dipole moment, it appears as a supplementary positive excess enthalpy to that inherently present from steric factors (evaluated from the mismatch in molecular size). Although for the two-component systems described in this work, excess properties, read Gibbs energy and enthalpy, of the liquid mixtures have not been reported in the literature, some evidence can be obtained by considering differences, particularly those between the R and FCC OD phases. Figure 11 shows the excess enthalpy differences between the OD phases and the liquid state (experimen-

tally available from the heat effect measured in the melting process) together with those between OD phases and low-temperature monoclinic phase. The values have been parametrized by using two-coefficient ( $\Delta_\phi^\gamma H_1$ ,  $\Delta_\phi^\gamma H_2$ ) Redlich–Kister polynomials (as eq 6 for the excess Gibbs energy difference). It should be kept in mind that excess enthalpy are the result of a number of successive arithmetical operations with data that have been determined in a direct experimental way or in an indirect manner, including extrapolations. Thus, some reserve must be exercised in drawing conclusions with regard to a desired fine-tuning. Nevertheless, within the described ubiquitous limiting conditions, some general trends can be achieved. It has been shown<sup>51–53</sup> that the geometric mismatch between the molecules of the two components of a given system plays a key role to account for the excess properties. Such a mismatch is parametrized by  $m$ , defined as the quotient between the difference between molar volumes of the components ( $\Delta V$ ) and their mean ( $V_m$ ), i.e.,  $m = \Delta V/V_m$ . As for methylchloromethane compounds, an additional role is played by the dipolar nature of the shared molecules.<sup>31</sup> More into specifics, it has been demonstrated that equimolar excess enthalpy of the OD phases ( $H^{\text{E,OD}}(X = 0.5)$ ) increases when the geometric mismatch increases and that an additional common value (ca.  $0.125 \text{ kJ}\cdot\text{mol}^{-1}$  for the equimolar composition) must be added for two-component systems sharing a polar and a nonpolar molecule (according to the effect that the authors called “dipole dilution”).<sup>31</sup> The mismatch parameters for OD phases of the two-component systems are calculated from the crystallographic results and are as follows: (i)  $\text{CCl}_4 + \text{CBr}_2\text{Cl}_2$ :  $m^{\text{FCC}} = 0.0584$ ;  $m^{\text{R}} = 0.0693$ ; (ii)  $\text{CBrCl}_3 + \text{CBr}_2\text{Cl}_2$ :  $m^{\text{FCC}} = 0.0327$ ;  $m^{\text{R}} = 0.0341$ . Although the established correlation cannot be quantitatively verified for the two-component systems of this work due to the lack of excess properties for the liquid mixtures, it is straightforward, as seen from Figure 11, that for both R and FCC OD phases, the highest deviation from ideal behavior corresponds to OD mixed crystals having the highest value of geometric mismatch parameter. In addition, assuming that deviation from ideality of liquid mixtures is smaller than for the OD phases (as it is commonly found), the excess enthalpy of OD phases for the polar + nonpolar system ( $\text{CCl}_4 + \text{CBr}_2\text{Cl}_2$ ) is noticeably higher than that which would correspond to the values of the  $m$  parameter, which means that the dipole dilution effect appears. We also note that in spite of uncertainties of the experimental excess enthalpy values, the asymmetry of the excess enthalpy functions (commonly expressed by the quotient of the two parameters of the Redlich–Kister expression for the excess enthalpy) is in line with the degree of asymmetry shown by the majority of the mixed crystal systems (ca.  $-0.2$ ).<sup>52–54</sup>

It is of interest to note the small excess Gibbs energy difference between the OD and M phases especially for the two-component system  $\text{CBr}_2\text{Cl}_2 + \text{CBrCl}_3$  (Table 4). Two factors are invoked to account for such effect. First, the close similarity in volume (difference is around 6.5%) and symmetry ( $C_{3v}$ ) between the molecules should generate resemblance between A–B interactions when compared to A–A or B–B. Second, the inherent disorder introduced by the substitution process.<sup>55</sup> Note that although the symmetry of both molecules ( $C_{3v}$ ) does not fulfill the symmetry requirements of the  $C2/c$  lattice site ( $T_d$ ), a symmetry simulation is generated by the appearance of an orientational disorder or by the change of the occupancy of the chlorine and bromine atoms as it has been demonstrated for both pure compounds as well as for mixed crystals by means of the structural refinement.

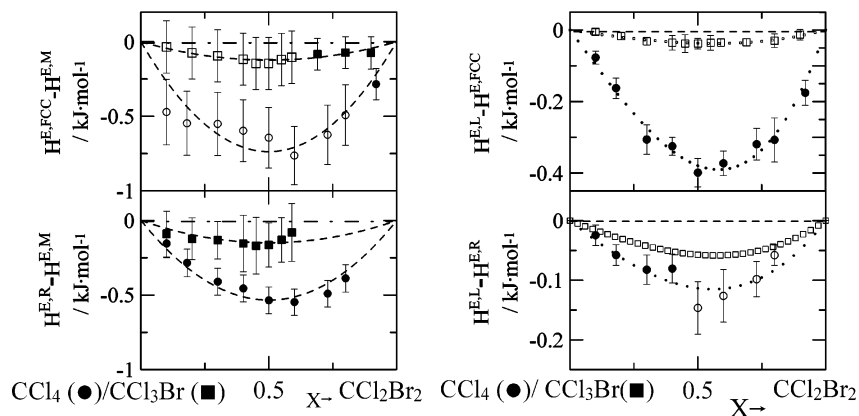


**Figure 11.** Excess enthalpy differences for the OD phases with respect to the liquid state (left panel) and for the monoclinic phase with respect to the OD phases (right panel) for the two-component systems  $\text{CCl}_4 + \text{CBr}_2\text{Cl}_2$  (circles) and  $\text{CBrCl}_3 + \text{CBr}_2\text{Cl}_2$  (squares). Full symbols correspond to direct experimental values while empty symbols correspond to values determined by means of eq. 1. Dashed lines are for the Redlich–Kister polynomials. The excess enthalpy difference  $H^{E,L} - H^{E,R}$  has been estimated by the using eq 1.

**TABLE 4:**  $\Delta_\alpha^\beta H_1 = H_1^\beta - H_1^\alpha$  and  $\Delta_\alpha^\beta H_2 = H_2^\beta - H_2^\alpha$  Parameters of the Redlich–Kister Polynomial for the Excess Enthalpy Difference between the Involved Phases in the  $\text{CCl}_4 + \text{CBr}_2\text{Cl}_2$  and  $\text{CBr}_2\text{Cl}_2 + \text{CBrCl}_3$  Two-Component Systems for Each of the Assessed Equilibria, Together with the Quotient  $H_1^{\text{OD}}/H_2^{\text{OD}}$  assuming Ideal Behavior in the Liquid State

equilibrium	$\alpha$	$\beta$	$\text{CCl}_4 + \text{CBr}_2\text{Cl}_2$			$\text{CBr}_2\text{Cl}_2 + \text{CBrCl}_3$		
			$\Delta_\alpha^\beta H_1 \text{ J}\cdot\text{mol}^{-1}$	$\Delta_\alpha^\beta H_2 \text{ J}\cdot\text{mol}^{-1}$	$H_2^{\text{OD}}/H_1^{\text{OD}}$	$\Delta_\alpha^\beta H_1 \text{ J}\cdot\text{mol}^{-1}$	$\Delta_\alpha^\beta H_2 \text{ J}\cdot\text{mol}^{-1}$	$H_2^{\text{OD}}/H_1^{\text{OD}}$
[FCC + L]	FCC	L	-1516	540	-0.356	-147	39	-0.265
[R + L]	R	L	-326	28	-0.086	-229	67	-0.293

Direct evidence for such a disorder has been obtained by heat capacity measurements<sup>3</sup> as well as by dielectric spectroscopy measurements,<sup>5,6</sup> both characterizing a glass transition at ca. 90 K associated to the freezing of the molecular disorder within the monoclinic phase. The linear dependence of the packing coefficient of the monoclinic phase as a function of the molar composition (Figure 10) goes along the ideal behavior of the low-temperature monoclinic mixed crystals.

## 5. Conclusions

The stable as well as the metastable parts of the two-component systems  $\text{CCl}_4 + \text{CBr}_2\text{Cl}_2$  and  $\text{CBrCl}_3 + \text{CBr}_2\text{Cl}_2$  have been determined by means of calorimetry and X-ray powder diffraction. The thermodynamic assessment coherently reproduces all the equilibria involved in both phase diagrams. Particularly noteworthy is the evidence for the common inferred metastable temperatures by means of the extrapolation of the two-phase equilibria, hardly obtained when the thermodynamic assessment is performed uniquely with one two-component system. These results suggest that the virtual character of such metastable transitions must be correlated with a physical reality. Thus, as it has been demonstrated in some previous works,<sup>6,8,34,41</sup> such transitions make appearance and acquire physical evidence when the extrapolation of high-pressure transition lines are considered. Then, detailed and coherent thermodynamic analyses of two-component systems can provided much more information than that typically obtained (as excess properties of the mixed crystals), in particular, for the pure components taking part in the binary system. In the present case, the existence of an orientational disordered high-pressure rhombohedral phase for the halogenomethane  $\text{CBr}_2\text{Cl}_2$  has been disclosed and a pressure-temperature topological diagram is inferred.

From the well-established crossed isopolymorphism we can conclude the existence of several isomorphism relationships (i) between the OD R stable phases of  $\text{CCl}_4$  and  $\text{CBrCl}_3$  and the OD R metastable (at normal pressure) phase of  $\text{CBr}_2\text{Cl}_2$ , (ii) between the OD FCC phase of  $\text{CCl}_4$  (metastable), the OD FCC

stable phase of  $\text{CBrCl}_3$  and OD FCC stable phase of  $\text{CBr}_2\text{Cl}_2$ , and (iii) between the low-temperature monoclinic phases of the three pure compounds involved in this study.

Interesting to note that this family of halogenomethane constitutes a remarkable case study because they are all molecules of almost identical geometry, with both polar and nonpolar species, with orientationally disordered phases and with glass transitions in the low-temperature “ordered” phase, which make a systematic comparison possible. As regard to the glass transition associated to the freezing of the disorder generated by the fractional occupancy of the chlorine and bromine atoms, dielectric spectroscopic and nuclear quadrupole resonance experiments have been undertaken around and below the glass transition temperature (ca. 90 K).

**Acknowledgment.** This work was supported by the Spanish Ministry of Education and Science (MEC) under project FIS2005-00975 and by the Catalan government by grant SGR2005-00535. We thank Dr. S. Coco at the Chemical Physics Department, University of Valladolid, for providing us with the pure  $\text{CBr}_2\text{Cl}_2$  used in this work.

## References and Notes

- (1) Timmermans, J. *J. Chim. Phys.* **1938**, 35, 331.
- (2) Parsonage, N. G.; Staveland, L. A. K. *Disorder in Crystals*; Clarendon: Oxford, 1978.
- (3) Ohta, T.; Yamamuro, O.; Matsuo, T. *J. Phys. Chem.* **1995**, 99, 2403.
- (4) Binbrek, O. S.; Lee-Dadswell, S. E.; Torrie, B. H.; Powell, B. M. *Mol. Phys.* **1999**, 96, 785.
- (5) Lee-Dadswell, S. E.; Torrie, B. H.; Binbrek, O. S.; Powell, B. M. *Physica B* **1998**, 241–243, 459.
- (6) Parat, B.; Pardo, L. C.; Barrio, M.; Tamarit, J. L.; Negrier, P.; Salud, J.; López, D. O.; Mondieig, D. *Chem. Mater.* **2005**, 17, 3359.
- (7) Rudman, R.; Post, B. *Science* **1966**, 154, 1009.
- (8) Barrio, M.; Pardo, L. C.; Tamarit, J. L.; Negrier, P.; López, D. O.; Salud, J.; Mondieig, D. *J. Phys. Chem. B* **2004**, 108, 11089.
- (9) Rudman, R. *J. Chem. Phys.* **1977**, 66, 3139.
- (10) Silver, L.; Rudman, R. *J. Phys. Chem.* **1970**, 74, 3134.
- (11) Rudman, R.; Post, B. *Mol. Cryst.* **1968**, 5, 95.
- (12) Rudman, R. *Solid State Commun.* **1979**, 29, 785.
- (13) Powers, R.; Rudman, R. *J. Chem. Phys.* **1980**, 72, 1629.

- (14) Cohen, S.; Powers, R.; Rudman, R. *Acta Cryst.* **1979**, *B35*, 1670.
- (15) Powers, R.; Rudman, R. *J. Chem. Phys.* **1980**, *72*, 1629.
- (16) More, M.; Baert, F.; Lefevre, J. *Acta Cryst.* **1977**, *B33*, 3681.
- (17) Dolling, G.; Powell, B. M.; Sears, V. F. *Mol. Phys.* **1979**, *37*, 1859.
- (18) Koga, Y.; Morrison, J. A. *J. Chem. Phys.* **1975**, *62*, 3359.
- (19) Hicks, J.; Hooley, J.; Stephenson, J. G. *J. Am. Chem. Soc.* **1944**, *66*, 1064.
- (20) Morrison, J. A.; Richards, E. L.; Sakon, M. *J. Chem. Thermodyn.* **1976**, *8*, 1033.
- (21) Arentsen, J. G.; Miltenburg, J. C. *J. Chem. Thermodyn.* **1972**, *4*, 789.
- (22) Rudman, R. *J. Mol. Struct.* **2001**, *569*, 157.
- (23) Pardo, L. C.; Barrio, M.; Tamarit, J. L.; López, D. O.; Salud, J.; Negrier, P.; Mondieig, D. *Phys. Chem. Chem. Phys.* **2001**, *3*, 2644.
- (24) Pardo, L. C.; Barrio, M.; Tamarit, J. L.; López, D. O.; Salud, J.; Negrier, P.; Mondieig, D. *Chem. Phys. Lett.* **1999**, *308*, 204.
- (25) Pardo, L. C.; Barrio, M.; Tamarit, J. L.; López, D. O.; Salud, J.; Negrier, P.; Mondieig, D. *Chem. Phys. Lett.* **2000**, *321*, 438.
- (26) Llanta, E.; Ando, K.; Rey, R. *J. Phys. Chem. B* **2001**, *105*, 7783.
- (27) Rey, R.; Pardo, L. C.; Llanta, E.; Ando, K.; López, D. O.; Tamarit, J. L.; Barrio, M. *J. Chem. Phys.* **2000**, *112* (17), 7505.
- (28) Llanta, E.; Rey, R. *Chem. Phys. Lett.* **2001**, *340*, 173.
- (29) Veglio, N.; Bermejo, F. J.; Pardo, L. C.; Tamarit, J. L.; Cuello, G. *J. Phys. Rev. E* **2005**, *72*, 031502.
- (30) Pardo, L. C.; Veglio, N.; Bermejo, F. J.; Tamarit, J. L.; Cuello, G. *J. Phys. Rev. B* **2005**, *72*, 014206.
- (31) Pardo, L. C.; Barrio, M.; Tamarit, J. L.; López, D. O.; Salud, J.; Oonk, H. A. *J. Chem. Mater.* **2005**, *17*, 6146.
- (32) Würflinger, A.; Pardo, L. C. *Z. Naturforsch.* **2002**, *57a*, 177.
- (33) Wenzel, U.; Schneider, G. M. *Mol. Cryst. Liq. Cryst. Lett. Sect.* **1982**, *72*, 255.
- (34) Barrio, M.; de Oliveira, P.; Céolin, R.; López, D. O.; Tamarit, J. L. *Chem. Mater.* **2002**, *14*, 851.
- (35) Bardelmeier, U.; Würflinger, A. *Thermochim. Acta* **1989**, *143*, 109.
- (36) Ventola, L.; Calvet, T.; Cuevas-Diarte, M. A.; Oonk, H. A. J.; Mondieig, D. *Phys. Chem. Phys. Chem.* **2004**, *6* (13), 3726.
- (37) Ballon, J.; Comparat, V.; Poux, J. *Nucl. Instrum. Methods* **1983**, *217*, 213.
- (38) Evain, M.; Deniard, P.; Jouanneaux, A.; Brec, R. *J. Appl. Cryst.* **1993**, *26*, 563.
- (39) Rodriguez-Carvajal, J.; Roisnel, T.; Gonzales-Platas, J. *FullProf Suite*, (April 2004 version); Laboratoire Le'on Brillouin, CEA-CNRS, CEN: Saclay, France.
- (40) Barrio, M.; Pardo, L. C.; Tamarit, J. L.; Negrier, Ph.; Salud, J.; López, D. O.; Mondieig, D. *J. Phys. Chem. B* **2006**, *110*, 12096.
- (41) Pardo, L. C.; Parat, B.; Barrio, M.; Tamarit, J. L.; López, D. O.; Salud, J.; Negrier, Ph.; Mondieig, D. *Chem. Phys. Lett.* **2005**, *402*, 408.
- (42) Oonk, H. A. *J. Phase Theory: The Thermodynamics of Heterogeneous Equilibria*; Elsevier Science Publishers: Amsterdam, 1981.
- (43) Daranas, D.; López, R.; López, D. O. *WINFIT.2.0*; Polytechnic University of Catalonia: Barcelona, 2000.
- (44) Jacobs, M. H. G.; Oonk, H. A. *J. LIQFIT, A Computer Program for the Thermodynamic Assessment of T-X Liquidus or Solidus Data*; Utrecht University: Utrecht, The Netherlands, 1990.
- (45) Oonk, H. A. J., Tamarit, J. L. "Measurement of Thermodynamic Properties of Multiple Phases", *Experimental Thermodynamics*, chapter 9; Weir, R. D., de Loos, T. W., Eds.; (IUPAC), Elsevier: Amsterdam, 2005; Vol. VII.
- (46) Calvet, T.; Cuevas-Diarte, M. A.; Haget, Y.; Mondieig, D.; Kok, I. C.; Verdonk, M. L.; Van Miltenburg, J. C.; Oonk, H. A. *J. Chem. Phys.* **1999**, *110*, 4841.
- (47) Rudman, R. *Mol. Cryst. Liq. Cryst.* **1970**, *6*, 427.
- (48) Kitaigorodsky, A. I. *Mixed Crystals*; Springer-Verlag: Berlin, 1984.
- (49) Miller, R. C.; Smyth, C. P. *J. Am. Chem. Soc.* **1957**, *79*, 20.
- (50) Bridgman, P. W. *Proc. Am. Acad. Arts Sci.* **1915**, *51*, 5; Bridgman, P. W. *Proc. Am. Acad. Arts Sci.* **1938**, *72*, 227.
- (51) Mondieig, D.; Espeau, P.; Robles, L.; Haget, Y.; Oonk, H. A. J.; Cuevas-Diarte, M. A. *J. Chem. Soc. Faraday Trans.* **1997**, *93* (18), 3343.
- (52) Oonk, H. A. *J. Pure Appl. Chem.* **2001**, *73* (5), 807.
- (53) López, D. O.; Salud, J.; Barrio, M.; Tamarit, J. L.; Oonk, H. A. *J. Chem. Mater.* **2000**, *12*, 1108.
- (54) Mondieig, D.; Rajabalee, F.; Metivaud, V.; Oonk, H. A. J.; Cuevas-Diarte, M. A. *Chem. Mater.* **2004**, *16*, 786.
- (55) Barrio, M.; López, D. O.; Tamarit, J. L.; Negrier, P.; Haget, Y. *J. Mater. Chem.* **1995**, *5*, 431.
- (56) Pardo et al., to be published.